HEAT TRANSFER AND PRESSURE LOSS CHARACTERIZATION IN A CHANNEL WITH DISCRETE FLUSH-MOUNTED AND PROTRUDING HEAT SOURCES

Y. Wang and K. Vafai
Department of Mechanical Engineering, The Ohio State University, Columbus, Ohio, USA

This work deals with an experimental investigation of the convective heat transfer and pressure loss in a rectangular channel with discrete flush-mounted and protruding heat sources. Six protruding obstacle heights, which represent the range of the dimensionless protrusion of $0 \leq h/H \leq 0.805$, are studied in this work. The temperatures on the heater surfaces and that of the fluid are collected, and data obtained at steady state are used to calculate the heat transfer coefficients, the Nusselt number, and the pressure loss coefficient. The results show that at lower Reynolds number, free convection cannot be neglected for cases where the discrete heat sources are flush-mounted on the channel floor. For cases of discrete protruding heat sources, heat transfer is dominated by forced convection and free convection can be ignored. The presence of the protruding heat sources distorts the flow in the channel, causing a substantial increase in heat transfer. Based on the experimental data, empirical correlations for the Nusselt number in terms of Reynolds number, and the dimensionless protruding height, are obtained for each heater by means of multiregression in the range $Re = 1{,}500–6{,}300$ and $h/H = 0.151–0.805$. The presence of the protruding heat sources increases the pressure loss dramatically. The results show that the pressure loss is dominated by the inertial effect. The results also quantify that the pressure loss coefficient, f, increases as the Reynolds number is decreased and/or h/H is increased. Based on the experimental data, an empirical relationship for the pressure loss coefficient in terms of Reynolds number and the dimensionless protruding height is obtained.

With the continued effort in compacting electronic equipment, the heat generated per unit volume in the electronic equipment has increased substantially, increasing further the average temperature of the equipment. Studies show that high temperature increases the failure rate and reduces the lifespan of electronic equipment [1]. Furthermore, if proper cooling methods are not employed, the temperature of the equipment will rise and affect operation. Therefore, cooling techniques are important for increasing the reliability and prolonging the lifespan of electronic equipment.

Several cooling techniques, such as forced convection, natural convection, and phase change, are commonly employed in practical applications. Among these techniques, forced convection with air as working medium is used more often than other techniques. This is due to its being a more cost-effective and safer technique while providing a moderate-size heat transfer coefficient.

Received 22 May 1998; accepted 29 May 1998.

Address correspondence to Prof. Kambiz Vafai, Department of Mechanical Engineering, The Ohio State University, Columbus, OH 43210, USA. E-mail: vafai.1@osu.edu

Experimental Heat Transfer, 12:1–16, 1999

0891-6152/99 $12.00 + .00

NOMENCLATURE

A_e	heat transfer area for the heater	H	height of channel
D_h	hydrodynamic diameter	k	conductivity
e_{av}	average error	L	streamwise length
f	pressure loss coefficient, Eq. (5)	Nu, $\overline{\text{Nu}}$	local and average Nusselt numbers, respectively, Eqs. (2) and (4)
g	gravitational constant		
Gr*	modified Grashof number, Eq. (7)	Δp	pressure drop
h	protrusion height	q	heat flux
h_c, $\overline{h}_c$	local and average convective heat transfer coefficients, respectively, Eqs. (1) and (3)	Re	Reynolds number, Eq. (6)
		β	thermal expansion coefficient
		ν	kinematic viscosity of the fluid

In order to enhance the forced convective heat transfer, several setups, such as porous obstacle arrangements [2], missing module arrangements, and barrier arrangements [3], can be utilized. Employing air as the cooling medium, Sparrow et al. [3] performed extensive experiments to investigate the forced convective heat transfer and the pressure drop in a rectangular channel with fully populated arrays of protruding modules. In their work, attention was given to the effect of barriers and missing modules on the heat transfer and pressure losses. It was found that the Nusselt number increases in the case of a missing block as well as when a barrier is present. It was also found that row-independent heat transfer coefficients were encountered after the fifth row. A study by Jubran et al. [4] also showed that the Nusselt number changed slightly after the fifth row of obstacles. Davalath and Bayazitoglu [5] developed a two-dimensional model for numerical prediction of viscous flow and the conjugate heat transfer (heat conduction in the blocks and convection in the fluid) between parallel plates with finite protruding block heat sources. The results showed that the protruding rectangular blocks changed the flow patterns in the channel considerably and thus affected the convective heat transfer.

Lehmann and Wirtz [6] carried out an experimental investigation of the effect of variations in the streamwise spacing and the streamwise length of the protruding heaters on convective heat transfer. In their study, the ratio of the streamwise length of the heaters to that of the spacing between the adjacent heaters was varied from 0 to 0.5. They found that Nusselt number variation was proportional to $\text{Re}^{0.65}$. McEntire and Webb [7] investigated a similar set and found that the average Nusselt number variation was proportional to $\text{Re}^{0.60}$. McEntire and Webb [7] also found that the average Nusselt number for the second- to fourth-row heaters were 40–90% higher than that of the leading heater. In very recent work, Young and Vafai [8–10] performed numerical and experimental studies on the convective heat transfer on the exposed surfaces of heated rectangular obstacles within a rectangular channel. The experiments were based on an entirely different setup and were performed for various Reynolds numbers and obstacle heights. It was found that the critical Reynolds number was within the range 4,000–4,500. Depending on the Reynolds number range, the exponent of the Reynolds number varied from 0.558 to 0.649 for $\text{Re} = 2{,}000$–$4{,}000$, and from 0.721 to 0.904 for $\text{Re} = 4{,}500$–$12{,}000$ [8–10].

Although considerable work has been done on forced convective cooling of electronic equipment, only a few articles report the pressure drop caused by the protruding discrete heat sources. The cited aspect constitutes one of the most prominent and fundamental configurations related to the electronic cooling. Furthermore, it appears that an empirical correlation for pressure loss coefficient has not been reported for this case. Determination of the optimum geometric parameters for enhancing the heat transfer process requires more investigations in this area. In the present work, an experimental investigation is performed on the convective heat transfer and pressure loss within a rectangular channel with protruding and flush-mounted discrete heat sources. Emphasis is placed on the convective heat transfer and pressure loss as well as their dependence on the Reynolds number and the protruding height.

EXPERIMENTAL SETUP AND PROCEDURE

A sketch of the experimental setup used in this work is shown in Figure 1. Air was drawn through the test section using a blower in the suction mode. The flow rate was adjusted through two valves. Two float flow meters with different flow-rate measurement ranges (5–25 and 25–110 SCFM) were used to meter the air flow rate. A thermocouple was placed at the entrance of the flow meter to measure the temperature necessary for correcting the flow meter readings.

The experimental channel consisted of a flow straighter, a test section, and an exit section. The flow straighter was a honeycomb that was 60 mm in length. The experimental test section was designed to allow a wide range of adjustment for the channel heights as well as the protruding heights of the heaters. The channel walls were constructed of clear acrylic ($k = 0.2$ W/m K). The channel was 765 mm in

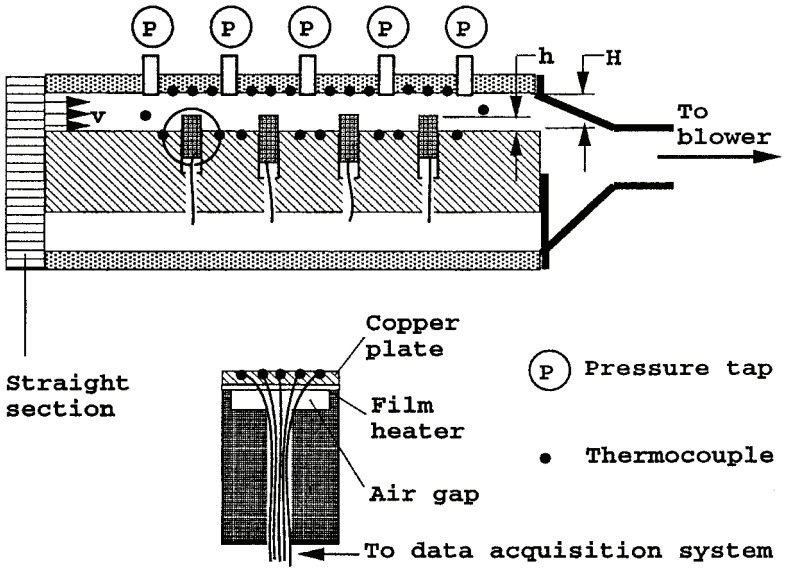

Figure 1. Schematic of the experimental system.

length and 204 mm in width. The channel height was adjustable within the range of a few millimeters to 80 mm. Four rectangular blocks were used in this investigation; they were 204 mm in length and 30 mm in width. The protruding heights of the blocks could be adjusted anywhere from 0 to 40 mm. The blocks were also made of clear acrylic. The blocks were separated in 95-mm intervals with the leading block being 203 mm downstream from the entrance. A copper plate of 204 mm by 30 mm by 1.7 mm was fixed on the top of each block. A thin-film resistance heater (Omega, Inc.) was attached to the bottom of each copper plate, resulting in four discrete heaters. For convenience, the leading heater is designated as 1 and successive heaters are referred to as heaters 2, 3, and 4. A 5-mm-deep slot was machined into the clear acrylic blocks, resulting in an insulative air gap between each block and the corresponding heater. The copper plates were polished with fine steel wool (#0000) in order to reduce the radiative losses. Shallow surface grooves, into which five thermocouples were mounted, were machined into the copper plates, and high-conductivity cement was filled in the grooves to reduce the disturbance.

The measured parameters were flow rate, temperature, and pressure drop as well as the voltage and current for the power supply. The voltage and current were recorded by a HP power supply. The flow rate was measured with floating flow meters (Aquamatic). Two flow meters were used for different flow rate measurement ranges. Five pressure taps were constructed on the upper plate of the test section. The distance between the adjacent pressure taps was 125 mm. The leading pressure tap was 205 mm from the entrance. A micropressure meter (Digital Manometer, Inc.) was used to measure the pressure drop in the channel. A switch allowed the pressure drop to be measured at different locations along the channel.

Fifty-seven type E thermocouples were employed. Of the 57 thermocouples, 2 were used to measure the temperature at the inlet and the outlet of the fluid, 15 were used to measure the temperature on the upper surface of the channel, 19 were used to measure the temperature on the lower surface of the channel, and of the remaining 20 thermocouples, 5 were mounted on the surface of each heater, covering a 5-mm width. The leading thermocouple was 2.9 mm from the leading edge of each heater.

To initiate the experiment, the channel and the protruding heights were first set at the prescribed values. The flow rate and the power supply output were then set at specified values. A constant-heat-flux boundary condition on the copper surfaces was maintained during the experiments. The temperatures were continuously monitored by a data acquisition system until steady-state conditions were reached. Depending on the flow rate, input power, channel height, and the protruding height of the obstacles, the time for reaching steady state varied from 50 to 430 min. Only the data collected at the steady state were used to calculate the heat transfer coefficients and friction coefficients.

EXPERIMENTAL RESULTS AND DISCUSSION

Data Reduction

In this work, six protruding heights ($h = 0, 6, 13, 20, 26, 32$ mm) were studied while the channel height was fixed at 39.75 mm. This translated to h/H variations

from 0 to 0.805. In these experiments, the radiation contribution can be neglected due to very small radiation coefficient and low heater surface temperature. The heat transfer coefficients were calculated from

$$h_c = \frac{q}{T_w - T_b} \tag{1}$$

where q is the heat flux and T_w and T_b are the heater surface and bulk fluid temperatures, respectively. The Nusselt number is calculated from

$$\mathrm{Nu} = \frac{h_c L}{k} \tag{2}$$

where L is the streamwise length of the heaters and k is the thermal conductivity of the fluid. In addition, the average heat transfer coefficient over a heater surface is calculated from

$$\overline{h_c} = \frac{\int_{A_e} h_c \, dA}{A_e} \tag{3}$$

where A_e is the heat transfer area for the heater. The average Nusselt number for the heater is in turn obtained from

$$\overline{\mathrm{Nu}} = \frac{\overline{h_c} L}{k} \tag{4}$$

Previous studies have shown that the friction pressure loss is quite small and the total pressure loss is dominated by the inertial loss in a channel containing protruding obstacles [3]. The pressure loss coefficient is defined as

$$f = \frac{\Delta p}{\frac{1}{2}\rho U^2} \tag{5}$$

where Δp is the pressure drop, U is the average velocity in the channel, and ρ is the density of the fluid. Finally, the Reynolds and modified Grashof numbers are calculated from

$$\mathrm{Re} = \frac{D_H U}{\nu} \tag{6}$$

and

$$\mathrm{Gr}^* = \frac{g\beta q H^4}{k\nu} \tag{7}$$

where D_H is the hydrodynamic diameter of the channel, ν is the kinematic viscosity, β the volumetric expansion coefficient, and H is the height of the channel.

Through an error analysis [11], the maximum uncertainty was found to be 2.0% for Nu, 8.5% for f, and 2.0% for both Reynolds number and Grashof number.

Flush-Mounted Case

Figure 2 shows the temperature distribution on the upper and lower surfaces of the channel. It can be seen that for the same input power, the temperature of the heater surfaces and the floor decreases as the Reynolds number is increased while the temperature distribution on the upper surface is changed slightly.

The temperature variation on each heater surface was quite small. The maximum difference appeared in heater 4 and was found to be less than 0.1 °C. This resulted an almost uniform Nusselt number for each heater, as can be seen in Figure 3. This was due to the low value of the Biot number for the copper plates, which was found to be about 0.002. Therefore, the heat transfer through the heated copper plates is dominated by convection and the temperature difference across each heater becomes negligible.

Due to the thermal boundary-layer development, the surface temperature of each heater increases along the flow direction. It should be noted that the average temperature on the surface of heater 4 was lower than that of heater 3. This is due to higher Nusselt number for heater 4 as compared to heater 3, which in turn initially suggests transition from laminar to turbulent flow. Assuming a uniform, constant-heat-flux boundary condition across the bottom surface of the channel, it can be shown that all the heaters are within the hydrodynamically and thermally developing region and that the flow is laminar throughout. However, it should be noted that the heater sources are discrete in this study and the uniform heat flux condition is not representative of the test section. Furthermore, preliminary

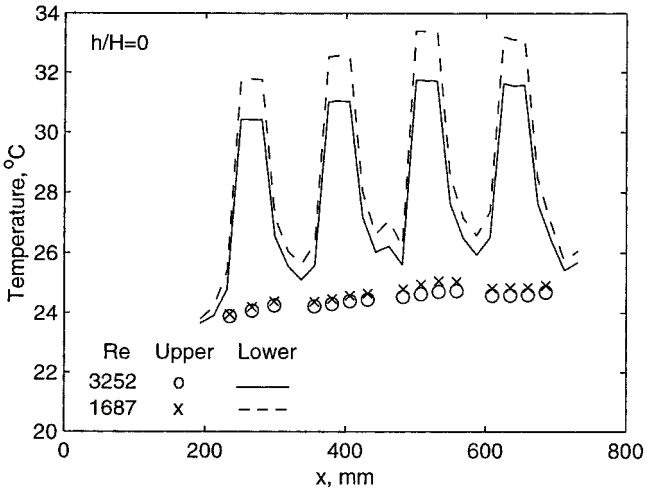

Figure 2. Temperature distribution on the upper and lower surfaces of the channel.

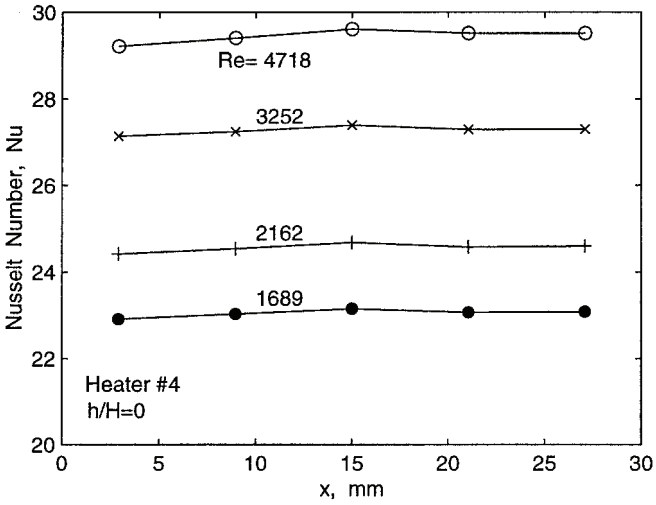

Figure 3. Nusselt number distribution along the flow direction for heater 4.

analysis shows that free convection plays a significant role in the heat transfer process and the total heat transfer is affected by both forced and free convection, with the free-convection contribution decreasing as the Reynolds number is increased. Due to the discontinuity of the heat sources, free convection would further affect the transition from laminar to turbulent flow. A study by McEntire and Webb [7] has indicated that a transition from laminar flow to turbulent flow appears at the third-row heater when the Reynolds number is larger than 5,000. The present work suggests that this transition may appear at a lower Reynolds number.

When both free and forced convection are significant, $\overline{Nu}/Re^{0.5}$ is usually a function of Gr^*/Re^2. Figure 4 is a plot of $\overline{Nu}/Re^{0.5}$ versus Gr^*/Re^2 for the experimental data obtained. It can be seen that $\overline{Nu}/Re^{0.5}$ increases as Gr^*/Re^2 is increased. Linear regression of the experimental data yields

$$\frac{\overline{Nu}}{Re^{0.5}} = 0.58\left(\frac{Gr^*}{Re^2}\right)^{0.13} \qquad \text{for the range } \frac{Gr^*}{Re^2} = 0.12\text{–}1.7 \tag{8}$$

or

$$\overline{Nu} = 0.58\, Gr^{*\,0.13}\, Re^{0.24} \qquad \text{for the range } Gr^*/Re^2 = 0.12\text{–}1.7 \tag{9}$$

The correlation given by Eq. (9) predicts the experimental data with an average error of 4.7%. Equation (8) is also plotted in Figure 4. It shows good agreement between the experimental data and the correlation presented.

Depending on the heater location, the exponent m of Re was found to be in the range 0.35–0.44 by McEntire and Webb [7]. Incropera et al. [12] found $m = 0.6$ for the first-row heater and $m = 0.78$ for the forth-row heater, with the value of m

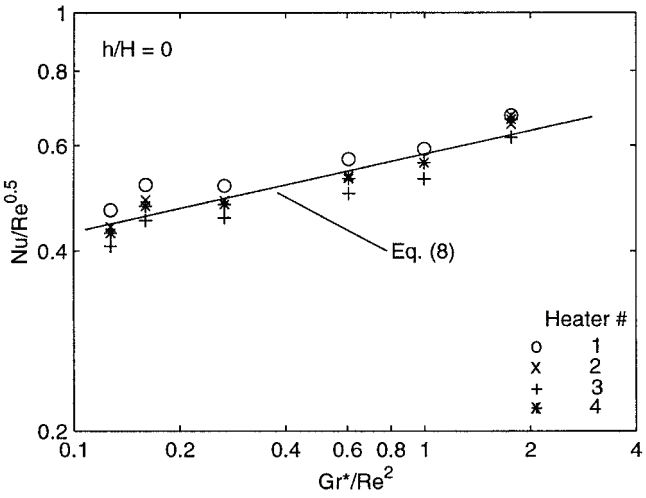

Figure 4. Average Nusselt number distribution for all the heaters.

between 0.6 and 0.78 for the second- and third-row heaters. The exponent difference between this work and that of Incropera et al. is significant. However, it should be noted that the results of this work were obtained in a thermally and hydrodynamically developing region and in a lower Reynolds number range. It also should be noted that the present results account for the mixed-convection regime, while those of Incropera [12] (1986) is based on a fully developed region and is conducted for a higher Reynolds number range without any significant mixed convection.

Discrete Protruding Case

The temperature distributions on the upper plate and the floor as well as on the heater surfaces corresponding to discrete protruding heaters are shown in Figure 5. The temperatures on the heater surfaces were smaller than that for the flush-mounted case for the same input heat, and increasing the protruding height caused the temperature to decrease further for the same Reynolds number, due to higher heat transfer coefficients.

The results show that with increasing protruding height, forced convection became the dominate mode of heat transfer, and free convection contributed only a small fraction to the total heat transfer. The free convection may be neglected for protruding heat source cases when $Re > 1{,}500$. The Nusselt number for heater 4 for two different protruding heights is plotted as a function of location in Figure 6. Once again, the Biot number was found to be small for the protruding heat sources ($Bi < 0.008$). Therefore, the temperature and Nusselt number variations were not significant for the heaters, as can be seen in Figure 6. It was found that an increase in the protruding height resulted in an increase in the Nusselt number for each heater. It was also found that the locations where the maximum Nusselt number occurred depended on the heater locations, Reynolds number, and

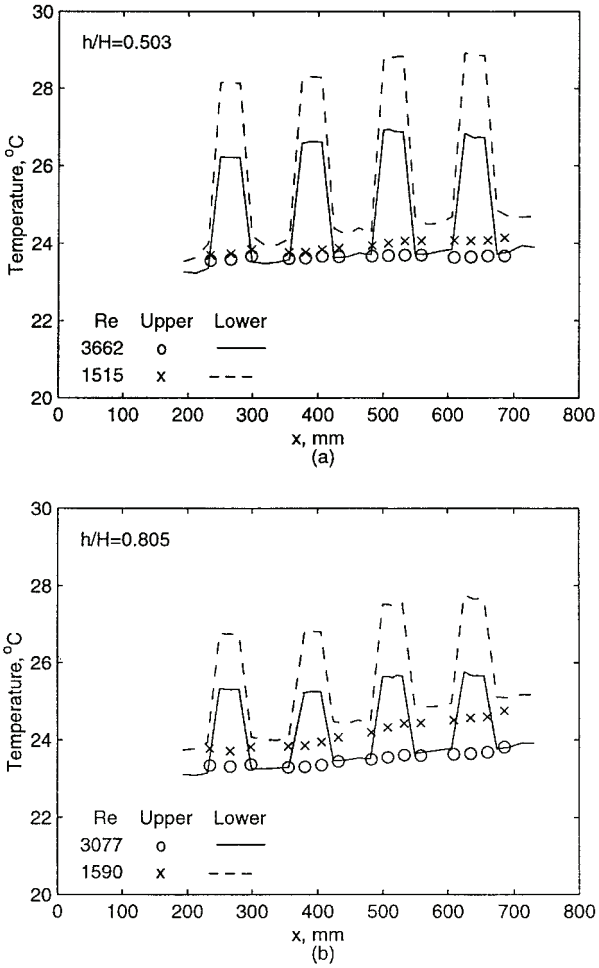

Figure 5. Temperature distribution on the upper plate and the floor including the protruding heater surfaces for: (*a*) $h/H = 0.503$; (*b*) $h/H = 0.805$.

the protruding height, h. For example, for $h = 13$ mm, 20 mm, and 26 mm, the maximum Nusselt number appeared at the leading edge for heater 2, while for heater 4, the maximum Nusselt number appeared at the center of the heater.

The differences in temperature and Nusselt number for each heater are indicative of the flow distortions within the channel due to the presence of the protruding blocks as well as small separated regions above the heater surfaces. The changes in the locations where the maximum or minimum Nusselt number appears suggests that the location and the shape of the separated regions may change with Reynolds number, the protruding height, and from one heater to another. The formation of the separated flow region has also been observed by others, as in a

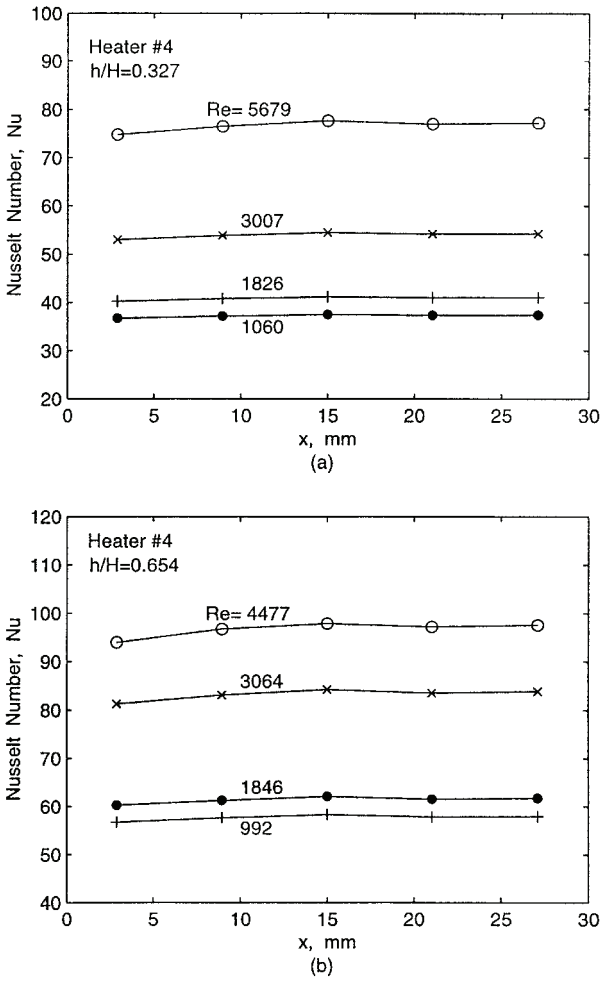

Figure 6. Nusselt number distribution along the flow direction for heater 4 for: (*a*) $h/H = 0.327$; (*b*) $h/H = 0.654$.

numerical study by Torok et al. [13]. Their results show that there is a small separated region just downstream of the leading edge of the first block.

The average Nusselt number, Nu, for each heating element and for different protrusion heights is plotted against the Reynolds number in Figures 7*a*–7*d*. As expected, it can be seen that the average Nusselt number increases with increasing Reynolds number for each h/H ratio. An exception to this trend occurred when the Reynolds number was around 1,200. At this Reynolds number, the average Nusselt number is larger than that of Reynolds number of 1,500 for all protruding heat source cases. This suggests that the critical Reynolds number, at which the transition from laminar flow to turbulent flow happens, occurs in the range from 1,200 to 1,600 in a rectangular channel with discrete protruding heat sources. A laser-Doppler velocity measurement in a channel with protruding blocks by Roller

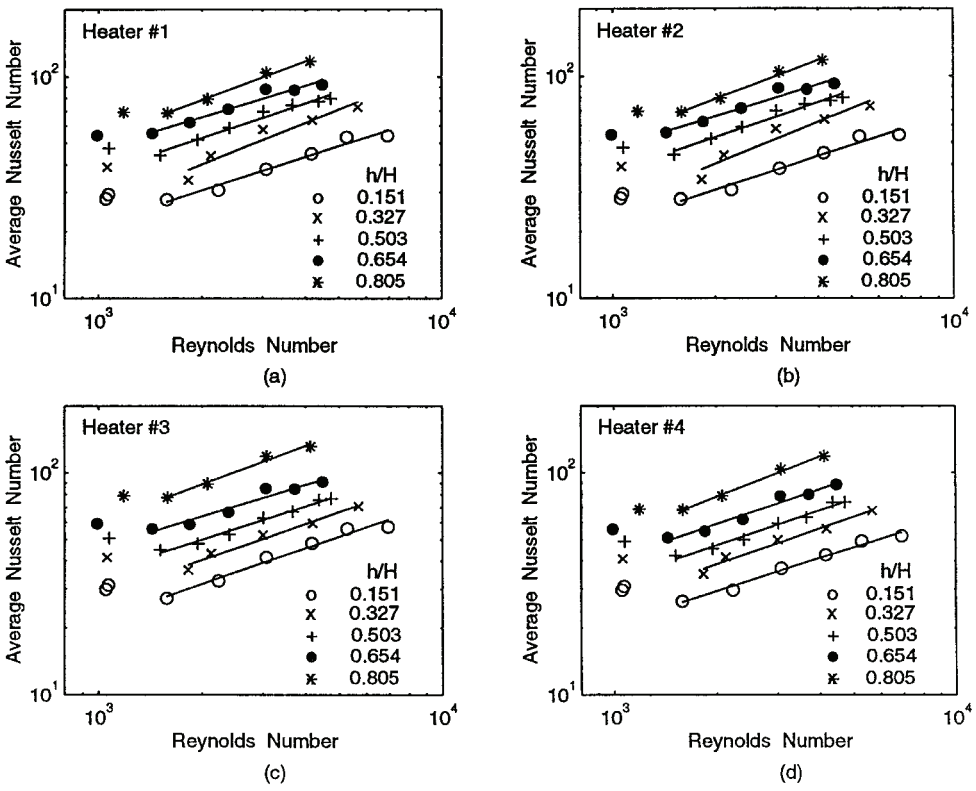

Figure 7. Average Nusselt number versus Reynolds number for: (*a*) heater 1; (*b*) heater 2; (*c*) heater 3; (*d*) heater 4.

et al. [14] indicated that the turbulence intensity increases substantially in the presence of protrusions in the range Re = 500–2,000, suggesting that the transition occurs within the cited Reynolds numbers. This means that the critical Reynolds number was between 500 and 2,000. A study conducted by Young and Vafai [9] shows that the critical Reynolds number is in the range 3,800–4,400. The difference in the critical Reynolds number between this work and that of Young and Vafai [9] can be attributed to the difference in the geometric parameters of the test sections and the heating boundary conditions. As can be seen in Figure 7, the protruding heights have a substantial effect on the average Nusselt number due to direct distortion of the flow field and consequently augmenting further the heat transfer rate with an increase in the height of the perturbation.

The average Nusselt number is correlated by the following equation when free convection is neglected:

$$\overline{\mathrm{Nu}} = A\,\mathrm{Re}^{m} \tag{10}$$

The constants A and m can be determined by a least-squares curve fit. This is similar to the form of correlation given by Roeller et al. [14]. The experimental

Table 1. Constants for Eq. (10)

h/H	0.151		0.327		0.503		0.654		0.805	
	A	m	A	m	A	m	A	m	A	m
Heater 1	0.648	0.500	0.336	0.629	0.972	0.526	1.791	0.474	0.952	0.581
Heater 2	0.532	0.537	0.630	0.547	1.095	0.503	1.722	0.475	1.121	0.575
Heater 3	0.701	0.491	0.646	0.538	0.890	0.522	1.138	0.519	0.851	0.594
Heater 4	0.676	0.503	0.494	0.582	0.603	0.581	0.991	0.545	0.987	0.583

data for $\mathrm{Re} < 1{,}500$, which appears to be within the laminar-flow regime, was excluded from the correlations. The results are illustrated in Table 1. The exponent m is in good agreement with the results obtained by Roeller et al. [14], McEntire and Webb [7], Lehmann and Wirtz [6], and Young and Vafai [9].

The small variations in the exponent for the Reynolds number for different heaters (Table 1) allows the attainment of a general correlation among Nu, Re, and (h/H) in the following form:

$$\overline{\mathrm{Nu}} = B\,\mathrm{Re}^{m}\left(\frac{h}{H}\right)^{n} \tag{11}$$

Utilizing multiparameter regression, the constants in Eq. (11) were obtained as shown in Table 2. The average relative errors, e_{av}, between the correlation given in Eq. (11) and the experimental data are also presented in Table 2. The results show that m varies from 0.515 to 0.545 and that n varies from 0.530 to 0.547. All the empirical correlations predict the experimental data with an average error less than 10.3%. The experimental data and the correlation results are both displayed in Figure 8. Once again, it can be seen that the heat transfer is strongly enhanced due to the existence of the discrete protruding heat sources.

Pressure Loss

The pressure loss for the flush-mounted case is relatively very small and can be calculated using Moody's friction factor diagram. The pressure loss distribution in the presence of the protruding heat sources for different protrusion heights and Reynolds numbers is shown in Figure 9. The pressure loss increases dramatically compared to that of the flush-mounted cases and, as can be seen in Figure 9, the pressure loss increases as the protruding height increases. The results also show

Table 2. Constants for Eq. (11)

Heater	A	m	n	e_{av}
1	1.47	0.528	0.547	6.14%
2	1.60	0.515	0.530	10.3%
3	1.48	0.516	0.534	7.9%
4	1.27	0.545	0.538	7.2%

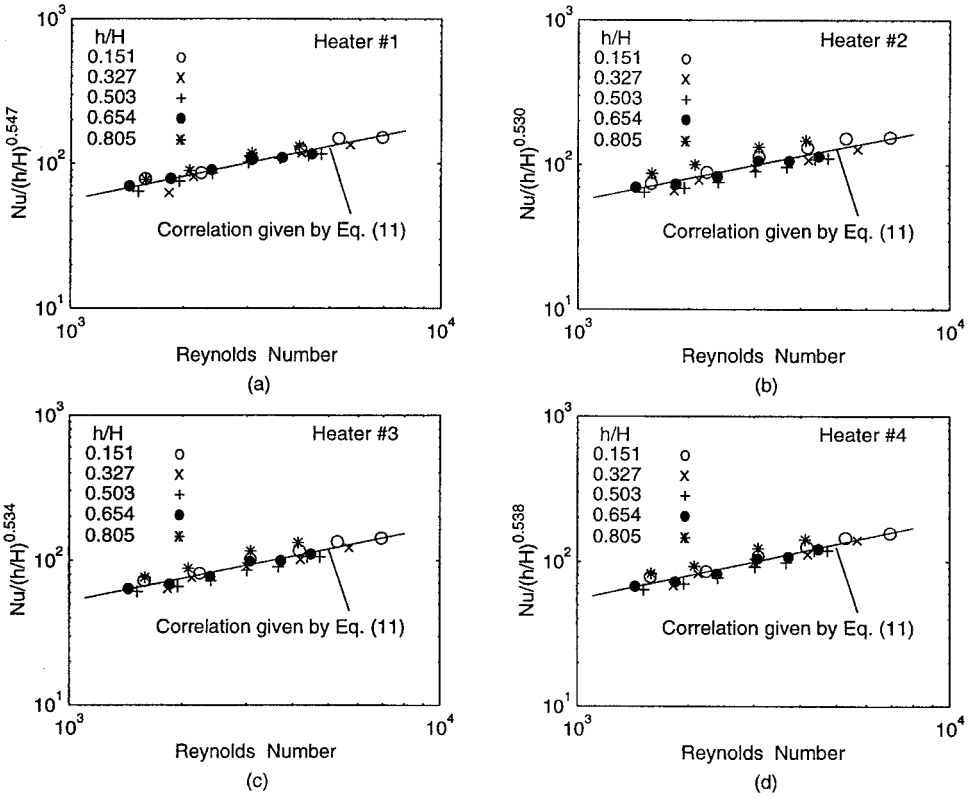

Figure 8. Average Nusselt number versus Reynolds number for different protrusion heights for: (*a*) heater 1; (*b*) heater 2; (*c*) heater 3; (*d*) heater 4.

that the pressure drop resulting from the leading protruding heater is relatively larger than pressure drop due to subsequent heaters, particularly for larger Reynolds numbers and protruding heights. The total pressure loss coefficient versus Reynolds number is plotted in Figure 10. As expected, the pressure loss coefficient, f, increases as the Reynolds number decreases and/or as h/H increases. Utilizing a least-squares fit, the total pressure loss coefficient for each protruding height is obtained as

$$f = A\,\mathrm{Re}^{-m} \tag{12}$$

The constants related to Eq. (12) are given in Table 3 for different protruding heights. Also shown in Table 3 are the average deviations from Eq. (12) as compared to the experimental data. As can be seen in Table 3, the exponent m varies from 0.423 to 0.489. The correlation given by Eq. (12) is displayed in Figure 10.

Multiparameter regression of the experimental data for the total pressure loss yields

$$f = 15.3\,\mathrm{Re}^{-0.454}\,e^{6.58(h/H)} \tag{13}$$

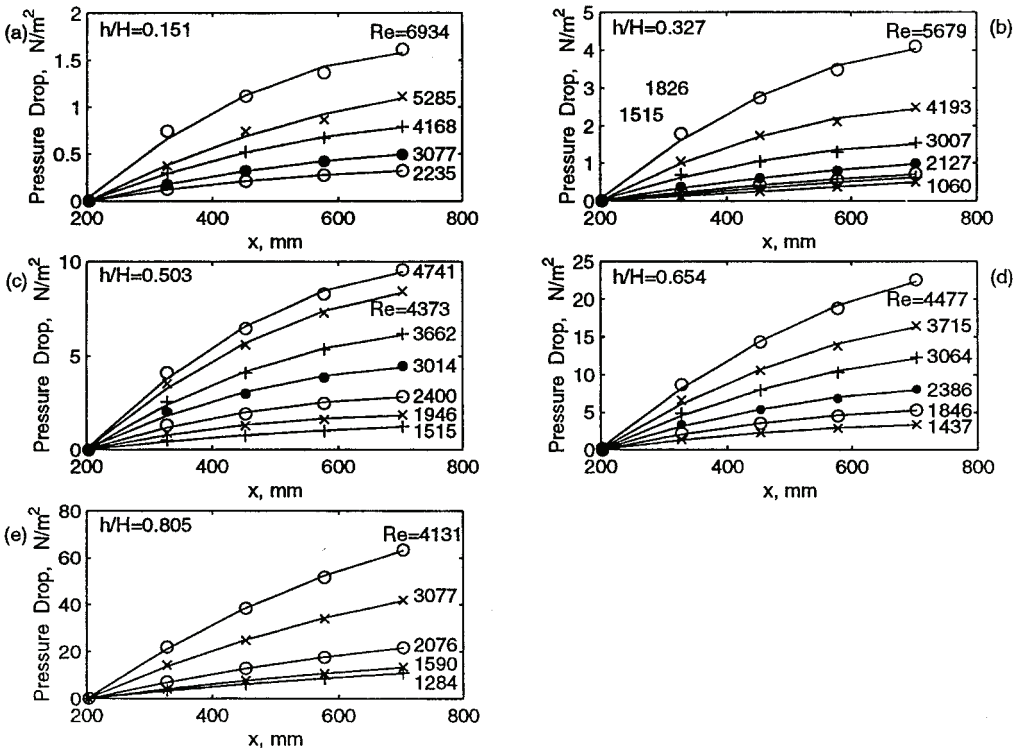

Figure 9. Pressure drop distribution for: (*a*) $h/H = 0.151$; (*b*) $h/H = 0.327$; (*c*) $h/H = 0.503$; (*d*) $h/H = 0.654$; (*e*) $h/H = 0.805$.

Equation (13) reproduces the experimental data with an average deviation of 6.9%, and it is plotted against the experimental data in Figure 11.

CONCLUSION

An experimental investigation of the convective heat transfer and pressure losses in a channel with discrete flush-mounted and protruding heat sources was presented in this work. The results reveal that for the flush-mounted discrete heat source case, free convection can take an important role in the total heat transfer process, leading to a possible mixed convective behavior. It is also found that the protruding heat sources distort the flow field substantially and cause the transition from laminar to turbulent flow to occur at a lower Reynolds number. Furthermore, the protruding heat sources enhance the forced convection significantly. Based on the experimental data, empirical correlations for predicting the average Nusselt number for mixed convection for the flush-mounted cases and forced convection for the protruding cases are obtained.

The heat transfer enhancement due to the protruding heat sources results in a substantial pressure loss. Measurement shows that the pressure loss for protruding heat source cases increases dramatically as compared to that for the flush-

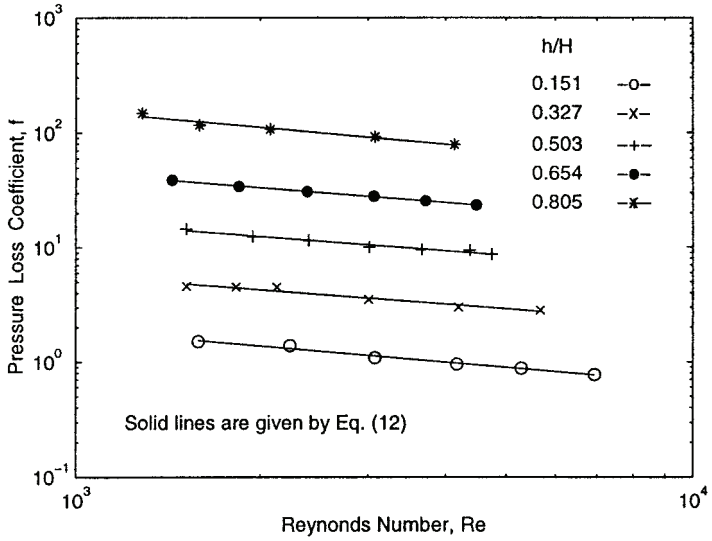

Figure 10. Pressure loss coefficient versus Reynolds number for different protrusion heights.

Table 3. Constants for Eq. (12)

h/H	0.151	0.327	0.503	0.654	0.805
A	49.0	106.0	315.0	603.9	4564.3
m	0.470	0.423	0.425	0.385	0.489
e_{av}	2.5%	4.1%	2.3%	1.1%	3.7%

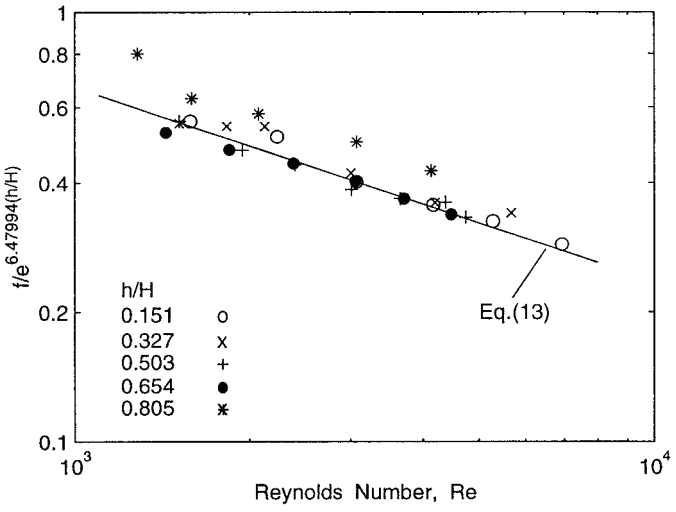

Figure 11. Unified pressure loss coefficient versus Reynolds number for different protrusion heights.

mounted case. An empirical correlation for the average pressure loss coefficient is also obtained in terms of the Reynolds number and the dimensionless protruding height.

REFERENCES

1. L. A. Nelson, K. S. Sekhon, and J. E. Fritz, Direct Heat Pipe Cooling of Semiconductor Devices, *Proc. 3rd Int. Heat Pipe Conf.*, pp. 373–376, 1978.
2. P. C. Huang and K. Vafai, Analysis of Forced Convection Enhancement in a Channel Using Porous Blocks, *J. Thermophys. Heat Transfer*, vol. 8, pp. 563–573, 1994.
3. E. M. Sparrow, J. E. Neithammer, and A. Chaboki, Heat Transfer and Pressure Drop Characteristics of Arrays of Rectangular Modules Encountered in Electronic Equipment, *Int. J. Heat Mass Transfer*, vol. 25, pp. 961–973, 1982.
4. B. A. Jubran, S. A. Swiety, and M. A. Hamdan, Convective Heat Transfer and Pressure Drop Characteristics of Various Array Configurations to Simulate the Cooling of Electric Modules, *Int. J. Heat Mass Transfer*, vol. 39, no. 16, pp. 3519–3529, 1996.
5. J. Davalath and Y. Bayazitoglu, Forced Convection Cooling Across Rectangular Blocks, *J. Heat Transfer*, vol. 109, pp. 321–328, 1987.
6. G. L. Lehmann and R. A. Wirtz, The Effect of Variations in Streamwise Spacing and Length on Convection from Surface Mounted Rectangular Components, *J. Electronic Package*, vol. 111, pp. 26–32, 1989.
7. A. B. McEntire and B. W. Webb, Local Forced Convective Heat Transfer from Protruding and Flush-Mounted Two-Dimensional Discrete Heat Sources, *Int. J. Heat Mass Transfer*, vol. 33, pp. 1521–1533, 1990.
8. T. J. Young and K. Vafai, Convective Flow and Heat Transfer in a Channel Containing Multiple Heated Obstacles, *Int. J. Heat Mass Transfer*, in press, 1998.
9. T. J. Young and K. Vafai, An Experimental Investigation of Forced Convective Characteristics of Arrays of Channel Mounted Obstacles, *ASME J. Heat Transfer*, in press, 1998.
10. T. J. Young and K. Vafai, Convective Cooling of Heated Obstacle in a Channel, *Int. J. Heat Mass Transfer*, in press, 1998.
11. R. J. Moffat, Describing the Uncertainties in Experimental Results, *Exp. Thermal Fluid Sci.*, vol. 1, pp. 3–17, 1988.
12. F. P. Incropera, J. S. Kerby, D. F. Moffat, and S. Ramadhyani, Convection Heat Transfer from Discrete Heat Sources in a Rectangular Channel, *Int. J. Heat Mass Transfer*, vol. 29, pp. 1051–1058, 1986.
13. D. Torok and R. Gronseth, Developing Flows in Narrow Channels Containing Heated Obstacles, *Int. J. Numer. Meth. Fluids*, vol. 8, pp. 1543–1561, 1988.
14. P. T. Roeller, J. Stevens, and B. W. Webb, Heat Transfer and Turbulent Flow Characteristics of Isolated Three-Dimensional Protrusions in Channel, *J. Heat Transfer*, vol. 113, pp. 597–603, 1989.